

RESEARCH

Open Access



# Finite volume method for solving the stochastic Helmholtz equation

Ruimin Xu<sup>1\*</sup> and Tingting Wu<sup>2</sup>

\*Correspondence:  
ruiminx@126.com

<sup>1</sup>School of Mathematics and Statistics, Qilu University of Technology (Shandong Academy of Sciences), Jinan, P.R. China  
Full list of author information is available at the end of the article

## Abstract

In this paper, we consider the linear finite volume method (FVM) for the stochastic Helmholtz equation, driven by white noise perturbed forcing terms in one-dimension. We first deduce the linear FVM for the deterministic Helmholtz problem. The dispersion equation is presented, and the error between the numerical wavenumber and the exact wavenumber is then analyzed. Comparisons between the linear FVM and the linear finite element method (FEM) are also made. The theoretical analysis and practical calculation indicate that the error of the linear FVM is half of that of the linear FEM. For the stochastic Helmholtz equation, convergence analysis and error estimates are given for the numerical solutions. The effects of the noises on the accuracy of the approximations are illustrated. Numerical experiments are provided to examine our theoretical results.

**Keywords:** Stochastic Helmholtz equation; White noise; Finite volume method

## 1 Introduction

In this paper, we consider the stochastic Helmholtz problem in one-dimension driven by an additive white noise forcing term (see [6, 15, 18])

$$\begin{cases} -\frac{d^2u}{dx^2} - k^2u(x) = g(x) + \dot{W}(x), & x \in (0, 1), \\ u(0) = 0, & u'(1) - ik u(1) = 0, \end{cases} \quad (1.1)$$

with the wavenumber  $k$ , where unknown  $u$  usually represents a pressure field in the frequency domain,  $i^2 = -1$ ,  $g$  is a deterministic real function with compact supports contained in  $I := [0, 1]$ , and  $\dot{W}(x)$  denotes the standard one-parameter family Brownian white noise that satisfies

$$\mathbb{E}[\dot{W}(x) \cdot \dot{W}(x')] = \delta(x - x'),$$

where  $\delta$  denote the usual Dirac  $\delta$ -function and  $\mathbb{E}$  the expectation. Following the standard stochastic theory of the white noise [23, 27], we have

$$\mathbb{E}[f(x)] = g(x) \quad \text{and} \quad \mathbb{V}[f(x)] = 1,$$

where  $\mathbb{V}$  is the variance operator. The stochastic Helmholtz equation has important applications in geophysics and medical science [4, 16, 18, 20, 26].

In recent years, finite difference methods (FDMs) and finite element methods (FEMs) have been developed to discretize the stochastic Helmholtz equation, for which the reader is referred to [5, 6, 8] and references cited therein. FDMs are easy to implement and locally conservative but not flexible to handle complex geometry. FEMs enjoy this flexibility. However, the main drawback of FEMs is its computational complexity and loss of the local conservation property. Finite volume methods (FVMs) possess the following advantages: the grid is flexible and the natural boundary conditions are easy to deal with; their implementation capability is comparable to that of finite difference methods; the mass conservation law is maintained, which is desirable in many engineering and science applications (see [10, 11, 13, 19] and references therein). It is worth mentioning that, for elliptic equations, although theoretical results indicate that both FVMs and FEMs enjoy the same optimal convergence order, the calculational effort of FVMs is usually less than that of FEMs, because of the asymmetry of their discrete schemes [19]. However, FVMs display many advantages when looking for the numerical solutions of computational fluid dynamics problems, because the mass conservation law is preserved [10]. The linear FVM for the stochastic Helmholtz equation in one-dimension will be developed in this paper. Furthermore, theoretical results and practical computations will illustrate that the FVM is more efficient than the FEM when solving the deterministic Helmholtz equation. In particular, the error of the linear FVM is only half of that of the linear FEM.

To numerically solve the stochastic Helmholtz equation, we should consider two issues: one is randomness, and the other is a high wavenumber. We turn to randomness first. The stochastic Helmholtz equation is a stochastic partial differential equation. As presented in [1, 7, 12], the difficulty in the error analysis of general numerical methods for a stochastic partial differential equation is the lack of regularity of its solution. Particularly, for the one-dimensional case, if  $\dot{W}$  corresponds to the white noise, it has been shown that the regularity estimates are usually very weak, and lead to low order error estimates [1]. Therefore, we first follow [1, 7, 12] to approximate the white noise by a piecewise constant process, which converts the stochastic Helmholtz equation into the deterministic Helmholtz equation. For other methods to discretize the white noise, the reader is referred to [27] and references therein. We then apply the linear FVM to the stochastic Helmholtz equation with discretized white noise forcing terms. For the case with a more regular noise, high-order FVMs will be discussed in our future work.

On the other hand, solving the deterministic Helmholtz equation numerically with large wavenumbers is still a challenging task. For many years, FDMs (see [17, 22, 24, 25] and the reference therein), FEMs (see [2, 3, 15]) and discontinuous Galerkin methods (DGs) (see [14]) have been widely used to discretize the deterministic Helmholtz equation with various boundaries. For large wavenumbers, the quality of the numerical results usually deteriorates as the wavenumber  $k$  increases, which is the so-called “pollution effect” of high wavenumbers [3, 15]. Moreover, due to this pollution effect, the wavenumber of the numerical solution is different from that of the exact solution, which is known as “numerical dispersion” [15]. Hence, for numerically solving the deterministic Helmholtz equation, two main issues should be focused on: one is the numerical dispersion which is closely related to the pollution error, while the other is the solver cost. So far, the “pollution term” of the error estimates, which is connected with the “pollution effect” of high wavenumbers, and the numerical dispersion have not been considered for FVMs.

This paper is organized as follows. In Sect. 2, we deduce the linear FVM for the deterministic Helmholtz problem in one-dimension, and then consider its solution’s existence and uniqueness. For the linear FVM, we establish its solution’s error estimates in  $H^1$ - and  $L_2$ -norm, then present its dispersion equation, and analyze the error between the numerical and exact wavenumbers. Comparisons between the linear FVM and FEM are also made in this section. Theoretical results indicate that the error for the linear FVM is half of that for the linear FEM. In Sect. 3, we study the approximation of (1.1) using discretized white noises. We also establish the regularity of the solution of the approximate problem and its error estimates in  $H^1$ -norm. In Sect. 4, we study the linear FVM of the stochastic Helmholtz equation with discretized white noise forcing terms, and obtain the  $H^1$  error estimates between the finite volume solutions and the exact solution of (1.1). In Sect. 5, three numerical experiments, including two for the deterministic Helmholtz problem and one for the stochastic Helmholtz equation, are given to demonstrate the efficiency and accuracy of the linear FVM. In particular, numerical results illustrate that, when solving the deterministic Helmholtz problem, the error for the linear FVM is only half of that for the linear FEM. Finally, Sect. 6 contains the conclusions of this paper.

## 2 The linear FVM for the deterministic Helmholtz equation in one-dimension

In this section, we deduce the linear FVM for the deterministic Helmholtz problem in one-dimension

$$\begin{cases} -\frac{d^2u}{dx^2} - k^2u(x) = g(x), & x \in (0, 1), \\ u(0) = 0, & u'(1) - iku(1) = 0. \end{cases} \tag{2.1}$$

We choose the trial and the test function spaces as linear finite element and piecewise constant function spaces, respectively. For the linear FVM, we consider its solution’s existence and uniqueness, and establish the error estimates. The dispersion equation is also presented, and the error between the numerical and exact wavenumbers is analyzed. Furthermore, we make comparisons between the linear FVM and FEM. Theoretical analysis indicates that the error for the linear FVM is half of that for the linear FEM.

We begin with introducing some useful notations. We denote by  $L^2(I)$  the space of all square-integrable complex-valued functions equipped with the inner product

$$(v, \omega) := \int_0^1 v(x)\bar{\omega}(x) dx, \quad \forall v, \omega \in L^2(I),$$

and the norm

$$\|\omega\|_0 := (\omega, \omega)^{\frac{1}{2}}, \quad \forall \omega \in L^2(I).$$

By  $H^1(I)$  we denote the Sobolev space

$$H^1(I) := \{u : u \in L^2(I) \text{ and } u' \in L^2(I)\}.$$

The norm of the space  $H^1(I)$  is defined as

$$\|u\|_1 := (\|u\|_0^2 + \|u'\|_0^2)^{\frac{1}{2}}, \quad \forall u \in H^1(I).$$

We also introduce the  $H^1$ -seminorm as

$$\|u\|_1 := \|u'\|_0, \quad \forall u \in H^1(I).$$

It follows from [15] that the Green's function of (2.1) can be presented as

$$G(x, s) = \frac{1}{k} \begin{cases} \sin(kx)e^{iks}, & 0 \leq x \leq s, \\ \sin(ks)e^{ikx}, & s \leq x \leq 1. \end{cases} \tag{2.2}$$

The solution  $u(x)$  of problem (2.1) exists for all  $k > 0$  and can be written as

$$u(x) = \int_0^1 G(x, s)g(s) ds.$$

In addition, Lemma 1 in [15] presents bounds of the exact solution and its derivatives given the data  $g$ .

**Lemma 2.1** *Let  $u \in H^2(I)$  be the solution to problem (2.1) for given data  $g \in L^2(I)$ . Then*

$$\|u\|_0 \leq \frac{1}{k} \|g\|_0, \quad \|u'\|_0 \leq \|g\|_0, \quad \|u''\|_0 \leq (1 + k) \|g\|_0.$$

### 2.1 Trial and test function spaces

In this subsection, we present the trial and the test function spaces for the linear FVM. We begin with discretizing the interval  $I$  into a grid  $T_h$  with nodes

$$0 = x_0 < x_1 < \dots < x_n = 1.$$

Denote the length of the element  $I_j := [x_{j-1}, x_j]$  by  $h_j = x_j - x_{j-1}$  and write  $h = \max_{1 \leq j \leq n} h_j$ . We assume the grid satisfies the quasi-uniformity condition  $h_j \geq \mu h$  ( $j = 1, 2, \dots, n$ ) for some positive constant  $\mu$ .

The trial space  $U_h$  is taken as the linear element space with respect to  $T_h$ , which consists of all the functions  $u_h$  satisfying

- (i)  $u_h \in C(I)$ ,  $u_h(0) = 0$  and
- (ii)  $u_h$  is linear on each  $I_j$  and is determined uniquely by its values at the endpoints of the element.

Obviously  $U_h$  is an  $n$ -dimensional subspace of  $H^1_E(I) := \{v : v \in H^1(I), v(0) = 0\}$ .

We next present the nodal basis functions for  $U_h$ . The basis function with respect to  $x_j$  is

$$\phi_j(x) = \begin{cases} 1 + \frac{x-x_j}{h_j}, & x_{j-1} \leq x \leq x_j, \\ 1 - \frac{x-x_j}{h_{j+1}}, & x_j \leq x \leq x_{j+1}, \\ 0, & \text{elsewhere,} \end{cases} \quad j = 1, 2, \dots, n-1, \tag{2.3}$$

and

$$\phi_n(x) = \begin{cases} 1 + \frac{x-x_n}{h_n}, & x_{n-1} \leq x \leq x_n, \\ 0, & \text{elsewhere.} \end{cases} \tag{2.4}$$

The functions  $\{\phi_j(x) : j = 1, 2, \dots, n\}$  form a basis of  $U_h$  and any  $u_h \in U_h$  has the following expression

$$u_h = \sum_{j=1}^n u_j \phi_j(x),$$

where  $u_j = u_h(x_j)$ . On the element  $I_j$  we have

$$u_h = u_{j-1}(1 - \xi) + u_j \xi, \quad \xi = \frac{x - x_{j-1}}{h_j}, \tag{2.5}$$

$$u'_h = (u_j - u_{j-1})/h_j, \quad x \in I_j, j = 1, 2, \dots, n. \tag{2.6}$$

We then present a dual grid  $T_h^*$  with nodes

$$0 = x_0 < x_{1/2} < x_{3/2} < \dots < x_{n-1/2} < x_n = 1,$$

where  $x_{j-1/2} = (x_{j-1} + x_j)/2$ ,  $j = 1, 2, \dots, n$ . The dual elements are  $I_0^* = [x_0, x_{1/2}]$ ,  $I_j^* = [x_{j-1/2}, x_{j+1/2}]$  ( $j = 1, 2, \dots, n - 1$ ), and  $I_n^* = [x_{n-1/2}, x_n]$ . Accordingly we choose the test function space  $V_h$  as the piecewise constant function (step function) space, which contains all the functions  $v_h \in L^2(I)$  satisfying

- (i)  $v_h(x) = 0$ , for  $x \in I_0^*$ , and
- (ii)  $v_h$  is a constant on each  $I_j^*$  ( $j = 1, 2, \dots, n$ ).

The basis functions of  $V_h$  are

$$\psi_j(x) = \begin{cases} 1, & x \in I_j^*, \\ 0, & x \in I - I_j^*, \end{cases} \quad j = 1, 2, \dots, n. \tag{2.7}$$

Any  $v_h \in V_h$  has the form

$$v_h = \sum_{j=1}^n v_j \psi_j(x),$$

where  $v_j = v_h(x_j)$ .

### 2.2 Variational formulation and linear FVM

We deduce the linear FVM for the deterministic problem (2.1) in this subsection. For this purpose, we first present the variational formulation of (2.1). A variational formulation of (2.1) can be obtained formally by multiplying the deterministic Helmholtz equation with  $v \in H_E^1(I)$ . After partial integration we then arrive at the variational problem as follows: Find a function  $u \in H_E^1(I)$  such that

$$a(u, v) = (g, v), \quad \forall v \in H_E^1(I), \tag{2.8}$$

where

$$a(u, v) := \int_0^1 [u'(x)\bar{v}'(x) - k^2 u(x)\bar{v}(x)] dx - iku(1)\bar{v}(1), \quad (g, v) := \int_0^1 g(x)\bar{v}(x) dx.$$

According to [15], the variational problem (2.8) has a unique weak solution. Applying Poincaré inequality, we obtain a continuity estimate for  $a(\cdot, \cdot)$ , namely

$$|a(u, v)| \leq (1 + k + k^2)|u|_1|v|_1, \quad \forall u, v \in H_E^1.$$

We turn to the FVM for solving (2.1). The linear FVM approximation to (2.1) is: Find  $u_h = \sum_{m=1}^n u_m \phi_m(x)$  such that

$$a(u_h, \psi_j) = (g, \psi_j), \quad j = 1, 2, \dots, n, \tag{2.9}$$

where

$$\begin{aligned} a(u_h, \psi_j) &= \int_a^b u'_h(x) [\delta(x - x_{j-1/2}) - \delta(x - x_{j+1/2})] dx - k^2 \int_{x_{j-1/2}}^{x_{j+1/2}} u_h(x) dx \\ &= \frac{u_j - u_{j-1}}{h_j} - \frac{u_{j+1} - u_j}{h_{j+1}} - \frac{k^2}{8} [(h_j u_{j-1} + h_{j+1} u_{j+1}) + 3(h_j + h_{j+1})u_j], \\ &\quad j = 1, 2, \dots, n - 1, \\ u_0 &= 0, \quad a(u_h, \psi_n) = \frac{u_n - u_{n-1}}{h_n} - \frac{k^2}{8} h_n (u_{n-1} + 3u_n) - iku_n. \end{aligned}$$

### 2.3 Existence and uniqueness

In this subsection, we establish the existence and uniqueness of the solution for the linear FVM (2.9).

First, for  $u_h \in U_h$  it follows from (2.6) that

$$|u_h|_1 = \left[ \int_0^1 u'_h \bar{u}'_h dx \right]^{\frac{1}{2}} = \left[ \sum_{j=1}^n (u_j - u_{j-1})(\bar{u}_j - \bar{u}_{j-1})/h_j \right]^{\frac{1}{2}}. \tag{2.10}$$

Next, we define an interpolation operator  $\Pi_h^* : H_E^1(I) \rightarrow V_h$  by

$$\Pi_h^* u = \sum_{j=1}^n u_j \psi_j, \quad \forall u \in H_E^1(I). \tag{2.11}$$

We then have the lemma as follows.

**Lemma 2.2** *As the homogeneous equation*

$$a(u, v) = 0, \quad \forall v \in H_E^1(I), \tag{2.12}$$

*admits only the trivial solution, there exists a constant  $\alpha > 0$  independent of the subspace  $U_h$  such that for sufficiently small  $kh$ ,*

$$\sup_{\omega_h \in U_h, |\omega_h|_1=1} |a(u_h, \Pi_h^* \omega_h)| \geq \alpha |u_h|_1, \quad \forall u_h \in U_h. \tag{2.13}$$

*Proof* We first rewrite  $a(u_h, \Pi_h^* \omega_h)$  as follows:

$$a(u_h, \Pi_h^* \omega_h) = a_1(u_h, \Pi_h^* \omega_h) - 2k^2(u_h, \Pi_h^* \omega_h),$$

where

$$a_1(u_h, \Pi_h^* \omega_h) = a(u_h, \Pi_h^* \omega_h) + 2k^2(u_h, \Pi_h^* \omega_h).$$

Below we examine the positive definiteness of  $a_1(u_h, \Pi_h^* u_h)$ . By (2.5),

$$\begin{aligned} k^2(u_h, \Pi_h^* u_h) &= k^2 \sum_{j=1}^{n-1} \bar{u}_j \left[ \int_{x_{j-1/2}}^{x_j} u_h dx + \int_{x_j}^{x_{j+1/2}} u_h dx \right] + k^2 \bar{u}_n \int_{x_{n-1/2}}^{x_n} u_h dx \\ &= k^2 \sum_{j=1}^{n-1} \bar{u}_j \left\{ h_j \int_{\frac{1}{2}}^1 [u_{j-1}(1-\xi) + u_j \xi] d\xi + h_{j+1} \int_0^{\frac{1}{2}} [u_j(1-\xi) + u_{j+1} \xi] d\xi \right\} \\ &\quad + k^2 \bar{u}_n h_n \int_{\frac{1}{2}}^1 [u_{n-1}(1-\xi) + u_n \xi] d\xi \\ &= \frac{3}{8} \sum_{j=1}^n u_j \bar{u}_j h_j + \frac{3}{8} \sum_{j=1}^{n-1} u_j \bar{u}_j h_{j+1} + \frac{1}{8} \sum_{j=1}^n u_{j-1} \bar{u}_j h_j + \frac{1}{8} \sum_{j=1}^n \bar{u}_{j-1} u_j h_j. \end{aligned}$$

Thus,  $k^2(u_h, \Pi_h^* u_h)$  is a real number. Furthermore, by (2.9) we have

$$\begin{aligned} a_1(u_h, \Pi_h^* u_h) &= \sum_{j=1}^{n-1} \bar{u}_j \left[ \frac{u_j - u_{j-1}}{h_j} - \frac{u_{j+1} - u_j}{h_{j+1}} \right] + \bar{u}_n \frac{u_n - u_{n-1}}{h_n} + k^2(u_h, \Pi_h^* u_h) - ik u_n \bar{u}_n \\ &= \sum_{j=1}^n \frac{(u_j - u_{j-1})(\bar{u}_j - \bar{u}_{j-1})}{h_j} + k^2(u_h, \Pi_h^* u_h) - ik u_n \bar{u}_n. \end{aligned}$$

Therefore,

$$\begin{aligned} \operatorname{Re} a_1(u_h, \Pi_h^* u_h) &= |u_h|_1^2 + k^2(u_h, \Pi_h^* u_h) \\ &= |u_h|_1^2 + k^2(u_h, u_h) + k^2(u_h, \Pi_h^* u_h - u_h) \\ &\geq |u_h|_1^2 + k^2 \|u_h\|_0^2 - k^2 \|u_h\|_0 \|\Pi_h^* u_h - u_h\|_0. \end{aligned} \tag{2.14}$$

By the interpolation theory, we get

$$\|\Pi_h^* u_h - u_h\|_0 \leq C_1 h |u_h|_1, \quad \forall u_h \in U_h. \tag{2.15}$$

Then we combine (2.14) with (2.15) to obtain

$$\begin{aligned} \operatorname{Re} a_1(u_h, \Pi_h^* u_h) &\geq |u_h|_1^2 + k^2 \|u_h\|_0^2 - C_1 k^2 h \|u_h\|_0 |u_h|_1 \\ &\geq \left(1 - \frac{C_1 k^2 h^2}{2}\right) |u_h|_1^2 + \frac{k^2}{2} \|u_h\|_0^2. \end{aligned}$$

Hence, for sufficiently small  $kh$ , one has

$$|a_1(u_h, \Pi_h^* u_h)| \geq \operatorname{Re} a_1(u_h, \Pi_h^* u_h) \geq \left(1 - \frac{C_1}{2} k^2 h^2\right) |u_h|_1^2, \quad \forall u_h \in U_h. \tag{2.16}$$

Now we turn to showing (2.13). Suppose by contradiction that there exists a sequence  $\{\tilde{u}_h\}, \tilde{u}_h \in U_h$ , satisfying

$$|\tilde{u}_h|_1 = 1, \quad \sup_{\omega_h \in U_h, |\omega_h|_1=1} |a(\tilde{u}_h, \Pi_h^* \omega_h)| \rightarrow 0 \quad \text{as } h \rightarrow 0. \tag{2.17}$$

Since  $H_E^1(I)$  is weakly sequentially compact,  $\{\tilde{u}_h\}$  has a subsequence (again written as  $\{\tilde{u}_h\}$ ) which converges weakly to some  $\tilde{u} \in H_E^1(I)$ . Take any  $\omega \in H_E^1(I)$  and write  $\Pi_h \omega$  as the interpolation projection of  $\omega$  onto the trial function space  $U_h$ . It is clear that  $\Pi_h^*(\omega - \Pi_h \omega) = 0$ . It follows from the interpolation theory that, when  $h$  is sufficiently small,

$$|\Pi_h \omega|_1 \leq |\omega|_1 + |\Pi_h \omega - \omega|_1 \leq |\omega|_1 + Ch|\omega|_2 \leq \|\omega\|_2. \tag{2.18}$$

By (2.17) we have

$$\begin{aligned} |a(\tilde{u}_h, \Pi_h^* \omega)| &= |a(\tilde{u}_h, \Pi_h^*(\Pi_h \omega))| \leq \sup_{\omega_h \in U_h, |\omega_h|_1=1} |a(\tilde{u}_h, \Pi_h^* \omega_h)| \cdot |\Pi_h \omega|_1 \\ &\leq C \sup_{\omega_h \in U_h, |\omega_h|_1=1} |a(\tilde{u}_h, \Pi_h^* \omega_h)| \cdot \|\omega\|_2 \rightarrow 0, \quad h \rightarrow 0. \end{aligned} \tag{2.19}$$

On the other hand, we next prove that  $|a(\tilde{u}_h, \Pi_h^* \omega - \omega)| \rightarrow 0, h \rightarrow 0$ . We first rewrite  $a(\tilde{u}_h, \Pi_h^* \omega - \omega)$  as follows:

$$a(\tilde{u}_h, \Pi_h^* \omega - \omega) = a(\tilde{u}_h, \Pi_h^* \omega) - a(\tilde{u}_h, \Pi_h \omega) + a(\tilde{u}_h, \Pi_h \omega - \omega). \tag{2.20}$$

It follows from the continuity of  $a(u, v)$  and the interpolation theory that

$$\begin{aligned} |a(\tilde{u}_h, \Pi_h \omega - \omega)| &\leq (1 + k + k^2) |\tilde{u}_h|_1 |\Pi_h \omega - \omega|_1 \\ &\leq C(1 + k + k^2) h |\tilde{u}_h|_1 |\omega|_2 \rightarrow 0, \quad h \rightarrow 0. \end{aligned} \tag{2.21}$$

In addition,

$$\begin{aligned} a(\tilde{u}_h, \Pi_h \omega) &= \int_0^1 \tilde{u}_h' (\overline{\Pi_h \omega})' dx - k^2 \int_0^1 \tilde{u}_h \overline{\Pi_h \omega} dx - ik \tilde{u}_n \bar{\omega}_n \\ &= \sum_{j=1}^n h_j \frac{\tilde{u}_j - \tilde{u}_{j-1}}{h_j} \frac{\bar{\omega}_j - \bar{\omega}_{j-1}}{h_j} - k^2 \int_0^1 \tilde{u}_h \overline{\Pi_h \omega} dx - ik \tilde{u}_n \bar{\omega}_n, \end{aligned} \tag{2.22}$$

$$\begin{aligned}
 a(\tilde{u}_h, \Pi_h^* \omega) &= \sum_{j=1}^{n-1} \bar{\omega}_j [\tilde{u}'_h(x_{j-\frac{1}{2}}) - \tilde{u}'_h(x_{j+\frac{1}{2}})] + \bar{\omega}_n \tilde{u}'_h(x_{n-\frac{1}{2}}) \\
 &\quad - k^2 \int_0^1 \tilde{u}_h \overline{\Pi_h^* \omega} \, dx - ik \tilde{u}_n \bar{\omega}_n \\
 &= \sum_{j=1}^n \tilde{u}'_h(x_{j-\frac{1}{2}}) (\bar{\omega}_j - \bar{\omega}_{j-1}) - k^2 \int_0^1 \tilde{u}_h \overline{\Pi_h^* \omega} \, dx - ik \tilde{u}_n \bar{\omega}_n \\
 &= \sum_{j=1}^n \frac{\tilde{u}_j - \tilde{u}_{j-1}}{h_j} (\bar{\omega}_j - \bar{\omega}_{j-1}) - k^2 \int_0^1 \tilde{u}_h \overline{\Pi_h^* \omega} \, dx - ik \tilde{u}_n \bar{\omega}_n. \tag{2.23}
 \end{aligned}$$

By (2.22) and (2.23), we get

$$a(\tilde{u}_h, \Pi_h^* \omega) - a(\tilde{u}_h, \Pi_h \omega) = k^2 (\tilde{u}_h, \Pi_h \omega - \Pi_h^* \omega) = k^2 (\tilde{u}_h, \Pi_h \omega - \omega) + k^2 (\tilde{u}_h, \omega - \Pi_h^* \omega).$$

It follows from the Cauchy inequality and the interpolation theory that

$$\begin{aligned}
 |a(\tilde{u}_h, \Pi_h^* \omega) - a(\tilde{u}_h, \Pi_h \omega)| &\leq k^2 \|\tilde{u}_h\|_0 \|\Pi_h \omega - \omega\|_0 + k^2 \|\tilde{u}_h\|_0 \|\omega - \Pi_h^* \omega\|_0 \\
 &\leq Ck^2 h \|\tilde{u}_h\|_0 \|\omega\|_2 \rightarrow 0, \quad h \rightarrow 0. \tag{2.24}
 \end{aligned}$$

Combining (2.20) and (2.21) with (2.24) yields

$$|a(\tilde{u}_h, \Pi_h^* \omega - \omega)| \rightarrow 0, \quad h \rightarrow 0. \tag{2.25}$$

We combine (2.19) with (2.25) to obtain

$$a(\tilde{u}_h, \omega) \rightarrow 0, \quad h \rightarrow 0. \tag{2.26}$$

For fixed  $\omega \in H_E^1(I)$ ,  $a(u, \omega)$  is a bounded linear functional on  $H_E^1(I)$ , which implies

$$a(\tilde{u}_h, \omega) \rightarrow a(\tilde{u}, \omega), \quad h \rightarrow 0. \tag{2.27}$$

By (2.26) and (2.27), we have

$$a(\tilde{u}, \omega) = 0, \quad \forall \omega \in H_E^1(I). \tag{2.28}$$

The assumption of the lemma then implies  $\tilde{u} = 0$ . So the sequence  $\tilde{u}_h$  converges weakly to zero. From the compactness of the imbedding of  $H_E^1(I)$  in  $L^2(I)$ , we know that  $\tilde{u}_h$  converges strongly to zero in  $L^2(I)$ , which gives

$$\|\tilde{u}_h\|_0 \rightarrow 0, \quad \text{as } h \rightarrow 0.$$

Furthermore, it follows from the Cauchy inequality and the interpolation theory that

$$|2k^2 (\tilde{u}_h, \Pi_h^* \tilde{u}_h)| \leq 2k^2 \|\tilde{u}_h\|_0 \|\Pi_h^* \tilde{u}_h\|_0 \leq Ck^2 \|\tilde{u}_h\|_0 \|\tilde{u}_h\|_0 \rightarrow 0, \quad h \rightarrow 0. \tag{2.29}$$

Finally, by (2.17) and (2.29), we conclude

$$\begin{aligned} |a_1(\tilde{u}_h, \Pi_h^* \tilde{u}_h)| &\leq |a(\tilde{u}_h, \Pi_h^* \tilde{u}_h)| + |2k^2(\tilde{u}_h, \Pi_h^* \tilde{u}_h)| \\ &\leq \sup_{\omega_h \in U_h, |\omega_h|_1=1} |a(\tilde{u}_h, \Pi_h^* \omega_h)| + Ck^2 \|\tilde{u}_h\|_0 \|\tilde{u}_h\|_0 \rightarrow 0, \quad h \rightarrow 0. \end{aligned} \tag{2.30}$$

This contradicts (2.16) and completes the proof. □

Based on Lemma 2.2, the following theorem indicates that the solution of (2.9) exists and is unique.

**Theorem 2.3** *If  $h$  is sufficiently small, then the linear FVM (2.9) has a unique solution for any given  $g \in L^2(I)$ .*

*Proof* By virtue of the well-known results in linear algebra, we only need to show that the homogeneous equation

$$a(u_h, \psi_j) = 0, \quad j = 1, 2, \dots, n - 1,$$

admits only the trivial solution, which follows from (2.13). □

### 2.4 Convergence order estimates

In this subsection, we present estimates for the error  $u - u_h$  in  $H^1$ - and  $L_2$ -norm for the linear FVM (2.9). The following theorem establishes an estimate for the error  $u - u_h$  in  $H^1$ -norm.

**Theorem 2.4** *Let  $u$  be solution of (2.1) satisfying  $u \in H^2(I)$  and  $u_h$  be the solution of the linear FVM (2.9). If  $h$  is sufficiently small, then*

$$|u - u_h|_1 \leq C(1 + k^2h)h|u|_2 \leq C(1 + k)(1 + k^2h)h\|g\|_0. \tag{2.31}$$

*Proof* Clearly, we have

$$a(u - u_h, \Pi_h^* \omega_h) = 0, \quad \forall \omega_h \in U_h. \tag{2.32}$$

Together with Lemma 2.2 and the interpolation theory, we observe that

$$|\Pi_h u - u_h|_1 \leq \frac{1}{\alpha} \sup_{\omega_h \in U_h, |\omega_h|_1=1} |a(u - \Pi_h u, \Pi_h^* \omega_h)|. \tag{2.33}$$

Let  $\omega_j = \omega_h(x_j)$ . Then we have  $\Pi_h^* \omega_h = \sum_{j=1}^n \omega_j \psi_j$  and

$$\begin{aligned} a(u - \Pi_h u, \Pi_h^* \omega_h) &= \sum_{j=1}^n (u - \Pi_h u)'_{j-1/2} (\bar{\omega}_j - \bar{\omega}_{j-1}) - k^2 \int_0^1 (u - \Pi_h u) \overline{\Pi_h^* \omega_h} dx \\ &\quad - ik[u(1) - \Pi_h u(1)] \bar{\omega}_n. \end{aligned} \tag{2.34}$$

By the Cauchy and Hölder inequalities and the definition of  $\Pi_h$ , we have that

$$\begin{aligned}
 & |a(u - \Pi_h u, \Pi_h^* \omega_h)| \\
 & \leq \left\{ \sum_{j=1}^n [(u - \Pi_h u)'_{j-1/2}]^2 \right\}^{\frac{1}{2}} \left\{ \sum_{j=1}^n |\bar{\omega}_j - \bar{\omega}_{j-1}|^2 \right\}^{\frac{1}{2}} + k^2 \|u - \Pi_h u\|_0 \|\Pi_h^* \omega_h\|_0. \quad (2.35)
 \end{aligned}$$

Below we present estimates for  $a(u - \Pi_h u, \Pi_h^* \omega_h)$  based on the above inequality, which leads to an estimate for  $|u_h - \Pi_h u|_1$ . It follows from (2.6) that

$$(u - \Pi_h u)'_{j-1/2} = u'_{j-1/2} - (u_j - u_{j-1})/h_j.$$

Furthermore, by the mean value theorem, there exists  $\xi_0 \in I_j$  such that

$$u'(\xi_0) = (u_j - u_{j-1})/h_j, \quad \text{i.e.,} \quad (u - \Pi_h u)'_{\xi_0} = 0.$$

Hence, we deduce that

$$(u - \Pi_h u)'_{j-1/2} = \int_{\xi_0}^{x_{j-1/2}} (u - \Pi_h u)'' dx = \int_{\xi_0}^{x_{j-1/2}} u'' dx,$$

which yields

$$\begin{aligned}
 & |(u - \Pi_h u)'_{j-1/2}|^2 \leq h \left[ \int_{\xi_0}^{x_{j-1/2}} (u'')^2 dx \right], \\
 & \left\{ \sum_{j=1}^n [(u - \Pi_h u)'_{j-1/2}]^2 \right\}^{\frac{1}{2}} \leq h^{1/2} |u|_2. \quad (2.36)
 \end{aligned}$$

Therefore, we have

$$\left\{ \sum_{j=1}^n [(u - \Pi_h u)'_{j-1/2}]^2 \right\}^{\frac{1}{2}} \left\{ \sum_{j=1}^n |\bar{\omega}_j - \bar{\omega}_{j-1}|^2 \right\}^{\frac{1}{2}} \leq h |u|_2 |\omega_h|_1. \quad (2.37)$$

In addition, by the interpolation theory we have

$$k^2 \|u - \Pi_h u\|_0 \leq C k^2 h^2 |u|_2, \quad (2.38)$$

$$\|\Pi_h^* \omega_h\|_0 \leq \|\Pi_h^* \omega_h - \omega_h\|_0 + \|\omega_h\|_0 \leq C |\omega_h|_1. \quad (2.39)$$

Combining (2.33) with (2.37)–(2.39) yields

$$|u_h - \Pi_h u|_1 \leq C(1 + k^2 h) h |u|_2.$$

Applying the interpolation theory in Sobolev spaces leads to

$$|u - \Pi_h u|_1 \leq Ch |u|_2.$$

The above two estimates and the regularity of  $u$  (see Lemma 2.1) lead to (2.31) and completes the proof.  $\square$

The above theorem indicates that the solution  $u_h$  of the linear FVM (2.9) approximates the solution  $u$  of (2.1) to first order in  $H^1$ -norm. Moreover, the term associated with  $k^2 h^2$  presents the pollution effect, which depends on the wavenumber  $k$ . The next theorem establishes an estimate for the error  $u - u_h$  in  $L_2$ -norm.

**Theorem 2.5** *Let  $u_h$  be the solution of (2.9), and  $u$  be the solution of (2.1) with  $u \in H^1_E(I) \cap W^{3,1}(I)$ . If  $k^2 h$  is small enough, then*

$$\|u - u_h\|_0 \leq C(1 + k)h^2 \|u\|_{3,1}. \tag{2.40}$$

*Proof* Let us introduce an auxiliary problem: For a given  $e = u - u_h$ , find  $\omega \in H^1_E(I)$  such that

$$a(v, \omega) = (v, e), \quad \forall v \in H^1_E(I). \tag{2.41}$$

It follows from Lemma 2.1 that the above problem possesses a unique solution satisfying

$$\|\omega\|_2 \leq 2(1 + k)\|e\|_0. \tag{2.42}$$

Combining (2.41) with (2.32) leads to

$$\begin{aligned} \|u - u_h\|_0^2 &= a(u - u_h, \omega) \\ &= a(u - u_h, \omega - \Pi_h \omega) + a(u - u_h, \Pi_h \omega) - a(u - u_h, \Pi_h^* \omega). \end{aligned} \tag{2.43}$$

By (2.31), (2.42) and the continuity of  $a(\cdot, \cdot)$ , we have

$$\begin{aligned} |a(u - u_h, \omega - \Pi_h \omega)| &\leq (1 + k + k^2) |u - u_h|_1 |\omega - \Pi_h \omega|_1 \\ &\leq C_1(1 + k)^2 (1 + k + k^2) (1 + k^2 h) h^2 |u|_2 \|u - u_h\|_0. \end{aligned} \tag{2.44}$$

Moreover, by a simple computation, we get

$$\begin{aligned} a(u - u_h, \Pi_h \omega) &= \sum_{j=1}^n \int_{x_{j-1}}^{x_j} (u - u_h)' dx \frac{\bar{\omega}_j - \bar{\omega}_{j-1}}{h_j} - k^2 \int_0^1 (u - u_h) \overline{\Pi_h \omega} dx \\ &\quad - ik [u(1) - u_h(1)] \bar{\omega}_n, \end{aligned} \tag{2.45}$$

$$\begin{aligned} a(u - u_h, \Pi_h^* \omega) &= \sum_{j=1}^n (u - u_h)'_{j-1/2} (\bar{\omega}_j - \bar{\omega}_{j-1}) - k^2 \int_0^1 (u - u_h) \overline{\Pi_h^* \omega} dx \\ &\quad - ik [u(1) - u_h(1)] \bar{\omega}_n. \end{aligned} \tag{2.46}$$

Thus there holds

$$\begin{aligned}
 & a(u - u_h, \Pi_h \omega) - a(u - u_h, \Pi_h^* \omega) \\
 &= \sum_{j=1}^n (u_j - u_{j-1} - h_j u'_{j-1/2}) \frac{\bar{\omega}_j - \bar{\omega}_{j-1}}{h_j} - k^2 \int_0^1 (u - u_h) [\overline{\Pi_h \omega} - \overline{\Pi_h^* \omega}] dx.
 \end{aligned} \tag{2.47}$$

Applying the Taylor expansion with an integral remainder yields

$$\begin{aligned}
 & \left| \sum_{j=1}^n (u_j - u_{j-1} - h_j u'_{j-1/2}) \frac{\bar{\omega}_j - \bar{\omega}_{j-1}}{h_j} \right| \\
 & \leq C_2 h^2 |u|_{3,1} |\omega|_{1,\infty} \leq C_2 (1+k) h^2 |u|_{3,1} \|u - u_h\|_0.
 \end{aligned} \tag{2.48}$$

In addition, we have

$$\begin{aligned}
 & \left| k^2 \int_a^b (u - u_h) [\overline{\Pi_h \omega} - \overline{\Pi_h^* \omega}] dx \right| \\
 & \leq \left| k^2 \int_a^b (u - u_h) [\overline{\Pi_h \omega} - \bar{\omega}] dx \right| + \left| k^2 \int_a^b (u - u_h) [\overline{\Pi_h^* \omega} - \bar{\omega}] dx \right| \\
 & \leq k^2 \|u - u_h\|_0 \|\Pi_h \omega - \omega\|_0 + k^2 \|u - u_h\|_0 \|\Pi_h^* \omega - \omega\|_0 \\
 & \leq [C_3 k^2 h^2 + C_4 k^2 h] (1+k) \|u - u_h\|_0^2.
 \end{aligned} \tag{2.49}$$

Combining (2.47)–(2.49) yields

$$\begin{aligned}
 & |a(u - u_h, \Pi_h \omega) - a(u - u_h, \Pi_h^* \omega)| \\
 & \leq C_2 (1+k) h^2 |u|_{3,1} \|u - u_h\|_0 + [C_3 k^2 h^2 + C_4 k^2 h] (1+k) \|u - u_h\|_0^2.
 \end{aligned} \tag{2.50}$$

By (2.43), (2.44), (2.50) and noting the imbedding relation  $W^{3,1}(I) \rightarrow H^2(I)$ , for sufficiently small  $k^2 h$ , we have

$$\|u - u_h\|_0^2 \leq \frac{C_1(1+k)(1+k+k^2)(1+k^2 h) + C_2}{1 - (C_3 k^2 h^2 + C_4 k^2 h)(1+k)} (1+k) h^2 \|u\|_{3,1} \|u - u_h\|_0.$$

This validates the estimate (2.40) and completes the proof. □

The above theorem indicates that in  $L_2$ -norm the solution  $u_h$  of the linear FVM (2.9) approximates the solution  $u$  of (2.1) to second order. Moreover, the term associated with  $kh^2$  presents the pollution effect, which depends on the wavenumber  $k$ .

### 2.5 Error analysis between the numerical and exact wavenumbers

In this subsection, we obtain the dispersion equation for the linear FVM (2.9) by a classical dispersion analysis, and provide an error analysis between the numerical and exact wavenumbers. Comparisons between the linear FVM and FEM are also made in this subsection, which indicate that the error for the linear FVM is half of that for the linear FEM.

Assuming that a uniform mesh is used, we then rewrite the linear FVM (2.9) for “interior” points  $x_j = j/n, 1 < j < n$  as

$$A_s(u_{j-1} + u_{j+1}) + A_o u_j = (g, \psi_j), \tag{2.51}$$

where

$$A_s = -\frac{1}{h} - \frac{1}{8}k^2h, \quad A_o = \frac{2}{h} - \frac{6}{8}k^2h.$$

Following the classical harmonic approach, we next insert the discrete expression of a plane wave  $u_j := e^{ikx_j}$  into equation (2.51). By a simple computation, we get the dispersion equation

$$2A_s \cos(kh) + A_o = 0. \tag{2.52}$$

Replacing variable  $k$  in the parameters  $A_s, A_o$  with the numerical wavenumber  $k^N$  in equation (2.52) yields an equation for the exact wavenumber  $k$  and the numerical wavenumber  $k^N$ , namely

$$k^N = \frac{1}{h} \sqrt{\frac{1 - \cos(kh)}{\frac{3}{8} + \frac{1}{8} \cos(kh)}}. \tag{2.53}$$

Based on the above equation, we will analyze the error between the numerical wavenumber  $k^N$  and the exact wavenumber  $k$  in the following proposition, when  $kh$  is small enough.

**Proposition 2.6** *For the linear FVM (2.9), if  $kh$  is small enough, then*

$$k^N = k + \frac{1}{48}k^3h^2 + \mathcal{O}(k^4h^3). \tag{2.54}$$

*Proof* Let  $\tau := kh$ , and denote

$$f_1(\tau) = 1 - \cos(\tau), \quad f_2(\tau) = \frac{3}{8} + \frac{1}{8} \cos(\tau).$$

Applying Taylor expansions for  $f_1(\tau)$  and  $\frac{1}{f_2(\tau)}$  at the point  $\tau = 0$  yields

$$f_1(\tau) = \frac{\tau^2}{2} - \frac{\tau^4}{24} + \mathcal{O}(\tau^6), \tag{2.55}$$

$$\frac{1}{f_2(\tau)} = 2 + \frac{1}{4}\tau^2 + \mathcal{O}(\tau^3). \tag{2.56}$$

In addition, from equation (2.53), we have

$$(k^N h)^2 = \frac{f_1(\tau)}{f_2(\tau)}.$$

Together with equations (2.55) and (2.56), we have

$$(k^N)^2 = k^2 + \frac{1}{24}k^4h^2 + \mathcal{O}(k^5h^3), \quad kh \rightarrow 0.$$

Based on the above equation, applying the Taylor expansion of the function  $\sqrt{1 + \tau}$  at the point  $\tau = 0$  leads to the conclusion of this proposition.  $\square$

The above proposition indicates that  $k^N$  approximates  $k$  to second order. Moreover, the term associated with  $k^3h^2$  presents the pollution effect, which depends on the wavenumber  $k$ . For the linear finite element method, a similar estimate for the relation  $k^N$  and  $k$  is obtained; see Remark 2.7.

*Remark 2.7* For the linear finite element method, if  $kh$  is sufficiently small, then

$$k^N = k + \frac{1}{24}k^3h^2 + \mathcal{O}(k^4h^3). \tag{2.57}$$

Equations (2.54) and (2.57) indicate that  $k^N$  approximates  $k$  to second order, for both the linear FVM and FEM. Moreover, the term associated with  $k^3h^2$  presents the pollution effect. We also find that the term associated with  $k^3h^2$  for the linear FVM is half of that for the linear FEM, when  $kh$  is small enough. However, when a uniform mesh is used, the quadratic finite volume method may not behave as well as the quadratic finite element method; see Remark 2.8.

*Remark 2.8* Assume that a uniform mesh is used. For the quadratic finite volume method, when  $kh$  is sufficiently small, we have

$$k^N = k - \frac{1}{192}k^3h^2 + \mathcal{O}(k^5h^4). \tag{2.58}$$

For the quadratic finite element method, when  $kh$  is small enough, we get

$$k^N = k + \frac{1}{1440}k^5h^4 + \mathcal{O}(k^7h^6). \tag{2.59}$$

We next present the normalized numerical phase and group velocities for the linear FVM, which are two important tools for measuring the numerical dispersion (see [17, 21]). In practice, the former is usually preferred. For a numerical method, when its normalized numerical phase velocity approximates 1 better, its numerical dispersion is smaller, and its accuracy is higher. Similar conclusions hold for the normalized numerical group velocity. For the convenience of analysis, let  $v$  be the velocity of propagation,  $\omega$  be the angular frequency,  $\lambda$  be the wavelength, and  $G$  be the number of gridpoints per wavelength, that is,  $G = \frac{\lambda}{h}$ . Since  $\lambda = \frac{2\pi v}{\omega}$  and  $k = \frac{\omega}{v}$ , we have  $kh = \frac{2\pi}{G}$ . Together with equation (2.53), we conclude that

$$\frac{k^N}{k} = \frac{G}{2\pi} \sqrt{\frac{1 - \cos(\frac{2\pi}{G})}{\frac{3}{8} + \frac{1}{8} \cos(\frac{2\pi}{G})}}. \tag{2.60}$$

The normalized numerical phase velocity, which is equivalent to  $\frac{k^N}{k}$  (cf. [9, 17]), is

$$\frac{V_{ph}^N}{v} = \frac{G}{2\pi} \sqrt{\frac{1 - \cos(\frac{2\pi}{G})}{\frac{3}{8} + \frac{1}{8} \cos(\frac{2\pi}{G})}}. \tag{2.61}$$

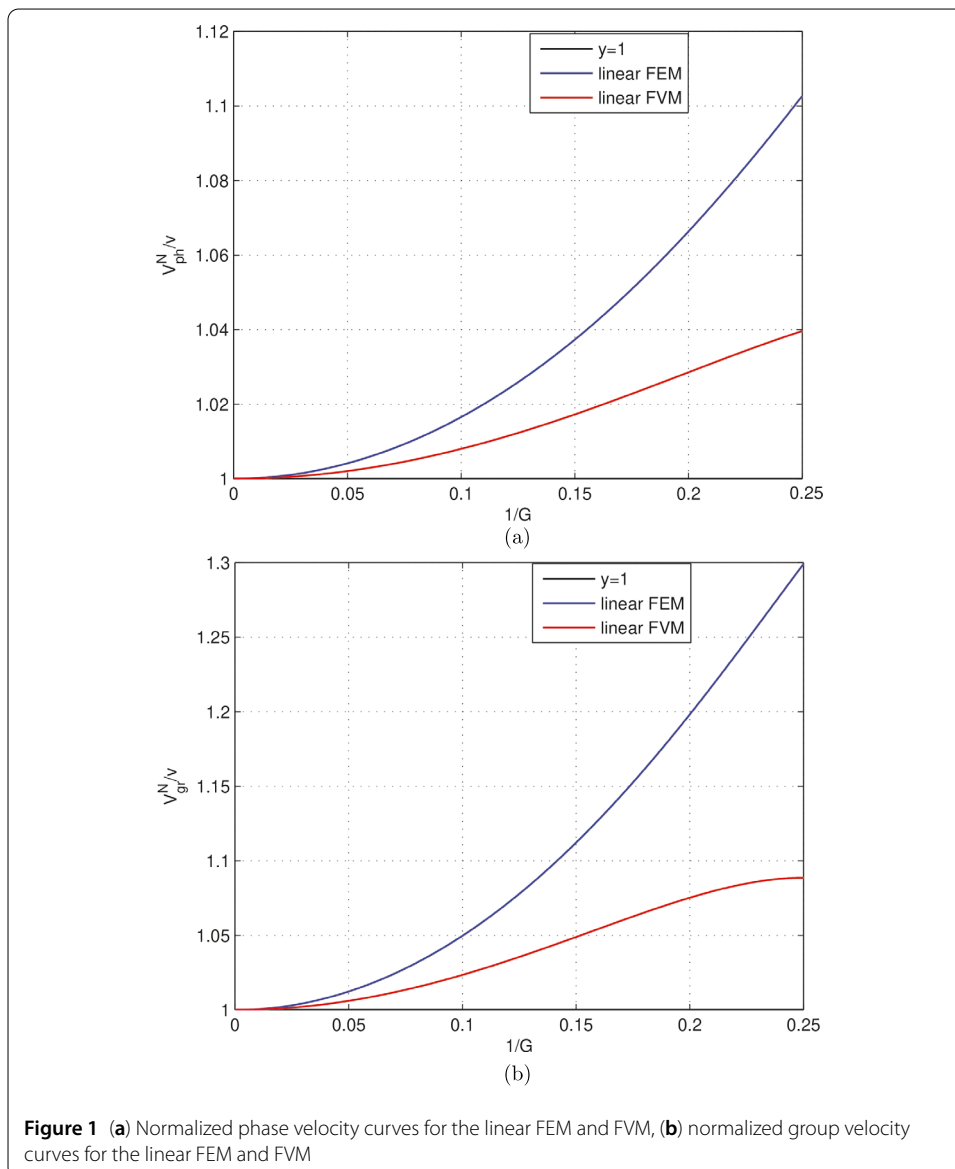
In addition, together with (2.54), we get

$$\frac{k^N}{k} = 1 + \frac{1}{48}k^2h^2 + \mathcal{O}(k^3h^3), \tag{2.62}$$

which indicates that the normalized numerical phase velocity approximates 1 to second order, when  $kh \rightarrow 0$ , and  $\frac{1}{48}k^2h^2$  is the main error term. Furthermore, the normalized numerical group velocity for the linear FVM is

$$\frac{V_{gr}^N}{v} = \frac{G}{4\pi} \frac{v}{V_{ph}^N} \frac{\frac{1}{2} \sin(\frac{2\pi}{G})}{[\frac{3}{8} + \frac{1}{8} \cos(\frac{2\pi}{G})]^2}. \tag{2.63}$$

Figure 1 shows the normalized phase and group velocity curves for the linear FVM and FEM, respectively. It is easy to find that the curves for the linear FVM approximate 1 better than those for the linear FEM. Specifically, the error between the normalized phase



velocity for the linear FVM and 1 is almost half of that for the linear FEM. The reason may be that, for the normalized phase velocity, the coefficient of the main error term for the linear FVM is half of that for the linear FEM (see (2.62)). Therefore, we expect that the linear FVM will enjoy higher numerical accuracy, when compared with the linear FEM. This will be illustrated by two numerical experiments in the next section.

### 3 The approximation problem for the stochastic Helmholtz equation in one-dimension

In this section, we first introduce an approximate problem of (1.1) by replacing the white noise  $\dot{W}$  by its piecewise constant approximation  $\dot{W}^s$ . Then we establish the regularity of the solution of the approximate problem and its error estimates.

We discretize the interval  $I$  in the same way as it is done in Sect. 2.1. Let

$$\xi_{I_j} := \frac{1}{\sqrt{h_j}} \int_{x_{j-1}}^{x_j} 1 dW(x),$$

for each interval  $I_j$ . It is well-known that  $\{\xi_{I_j}\}$  is a family of independent identically distributed normal random variables with mean 0 and variance 1 (see [23]). Then the piecewise constant approximation to  $\dot{W}(x)$  is given by

$$\dot{W}^s(x) = \sum_{j=1}^n h_j^{-\frac{1}{2}} \xi_{I_j} \chi_{I_j}(x), \tag{3.1}$$

where  $\chi_{I_j}$  is the characteristic function of  $I_j$ . It is easy to see that  $\dot{W}^s(x) \in L^2(I)$ . However, the following lemma shows that the  $L_2$ -norm  $\|\dot{W}^s\|_0$  of  $\dot{W}^s$  is unbounded as  $h \rightarrow 0$ .

**Lemma 3.1** *There holds*

$$h^{-1} \leq E(\|\dot{W}^s\|_0^2) \leq \frac{1}{\mu} h^{-1}. \tag{3.2}$$

*Proof* It is easy to see that

$$\|\dot{W}^s\|_0^2 = \sum_{I_j \in T_h} \int_{x_{j-1}}^{x_j} (h_j^{-\frac{1}{2}})^2 \xi_{I_j}^2 dx = \sum_{I_j \in T_h} \xi_{I_j}^2.$$

Therefore, we have that

$$E(\|\dot{W}^s\|_0^2) = \sum_{I_j \in T_h} E(\xi_{I_j}^2) = \sum_{I_j \in T_h} 1 = \sum_{j=1}^n h_j \cdot \frac{1}{h_j}.$$

By using the quasi-uniformity condition  $h_j \geq \mu h$  ( $j = 1, 2, \dots, n$ ), we come to the conclusion of this lemma. □

Replacing  $\dot{W}(x)$  by  $\dot{W}^s(x)$  in (1.1), we have the following stochastic Helmholtz equation with a discretized white noise forcing term:

$$\begin{cases} -\frac{d^2 u^s}{dx^2} - k^2 u^s(x) = g(x) + \dot{W}^s(x), & x \in (0, 1), \\ u^s(0) = 0, & \frac{du^s(1)}{dx} - ik u^s(1) = 0. \end{cases} \tag{3.3}$$

The variational problem of (3.3) is as follows: Find a function  $u^s \in H_E^1(I)$  such that

$$a(u^s, v) = (g, v) + (\dot{W}^s, v), \quad \forall v \in H_E^1(I). \tag{3.4}$$

As  $\dot{W}^s \in L^2(I)$ , it follows from [15] that (3.4) has a unique solution  $u^s$ . We then establish an estimate for the error  $u - u^s$ , where  $u$  is the solution of (1.1).

**Lemma 3.2** *There is a unique solution  $u^s \in H^2(I)$  of problem (3.3) which satisfies*

$$E(\|u^s\|_2^2) \leq C_5 h^{-1}, \tag{3.5}$$

where  $C_5$  is a positive constant independent of  $h$ .

*Proof* It follows from Lemma 2.1 that

$$\begin{aligned} \|u^s\|_2^2 &= \|u^s\|_0^2 + \|(u^s)'\|_0^2 + \|(u^s)''\|_0^2 \\ &\leq 2 \left[ \frac{1}{k^2} + 1 + (1+k)^2 \right] [\|g\|_0^2 + \|\dot{W}^s\|_0^2]. \end{aligned} \tag{3.6}$$

By (3.6) and (3.2), we come to the desired result. □

Next we estimate the error between the weak solution  $u$  of (1.1) and its approximation  $u^s$ . To this end, we present the solution  $u$  of (1.1) and the solution  $u^s$  of (3.3) by the Green function (2.2) as

$$u(x) = \int_0^1 G(x, y)g(y) dy + \int_0^1 G(x, y)\dot{W}(y) dy, \tag{3.7}$$

$$u^s(x) = \int_0^1 G(x, y)g(y) dy + \int_0^1 G(x, y)\dot{W}^s(y) dy. \tag{3.8}$$

We then establish the regularity of the Green function  $G(x, s)$  and  $\frac{\partial G(x, s)}{\partial x}$  defined in (2.2) in the following lemma, which will play an important role in the error estimate between  $u$  and  $u^s$ .

**Lemma 3.3** *There hold*

$$\int_0^1 |G(x, y) - G(x, z)|^2 dx \leq \left( \frac{12}{k^2} + 6k^2 \right) (y - z)^2, \quad \forall y, z \in I, \tag{3.9}$$

$$\int_0^1 \left| \frac{\partial G(x, y)}{\partial x} - \frac{\partial G(x, z)}{\partial x} \right|^2 dx \leq (3k^4 + 4) |y - z|, \quad \forall y, z \in I. \tag{3.10}$$

*Proof* Assume that  $0 \leq y < z \leq 1$ . We first prove that (3.9) holds. Obviously, we have

$$\begin{aligned} \int_0^1 |G(x, y) - G(x, z)|^2 dx &= \int_0^y |G(x, y) - G(x, z)|^2 dx + \int_y^z |G(x, y) - G(x, z)|^2 dx \\ &\quad + \int_z^1 |G(x, y) - G(x, z)|^2 dx \\ &= \text{I} + \text{II} + \text{III}. \end{aligned}$$

By (2.2), we get that

$$I = \int_0^y \frac{1}{k^2} \sin^2(kx) |e^{iky} - e^{ikz}|^2 dx \leq 2k^2(y - z)^2, \tag{3.11}$$

$$III = \int_z^1 \left| \frac{1}{k} \sin(ky)e^{ikx} - \frac{1}{k} \sin(kz)e^{ikx} \right|^2 dx \leq k^2(y - z)^2. \tag{3.12}$$

Similarly, we obtain

$$\begin{aligned} II &= \int_y^z \left| \frac{1}{k} \sin(ky)e^{ikx} - \frac{1}{k} \sin(kx)e^{ikz} \right|^2 dx \\ &= \frac{1}{k^2} \int_y^z \left| \sin(ky)e^{ikx} - \sin(ky)e^{iky} + \sin(ky)e^{iky} \right. \\ &\quad \left. - \sin(kx)e^{iky} + \sin(kx)e^{iky} - \sin(kx)e^{ikz} \right|^2 dx \\ &\leq \left( \frac{12}{k^2} + 3k^2 \right) |z - y|^3. \end{aligned} \tag{3.13}$$

Combining (3.11) and (3.13) with (3.12) yields (3.9).

Below we prove (3.10). By (2.2), we have that

$$\frac{\partial G(x, s)}{\partial x} = \begin{cases} \cos(kx)e^{iks}, & 0 \leq x \leq s, \\ i \sin(ks)e^{ikx}, & s \leq x \leq 1. \end{cases} \tag{3.14}$$

Arguing as before, we have

$$\begin{aligned} \int_0^1 \left| \frac{\partial G(x, y)}{\partial x} - \frac{\partial G(x, z)}{\partial x} \right|^2 dx &= \int_0^y \left| \frac{\partial G(x, y)}{\partial x} - \frac{\partial G(x, z)}{\partial x} \right|^2 dx \\ &\quad + \int_y^z \left| \frac{\partial G(x, y)}{\partial x} - \frac{\partial G(x, z)}{\partial x} \right|^2 dx \\ &\quad + \int_z^1 \left| \frac{\partial G(x, y)}{\partial x} - \frac{\partial G(x, z)}{\partial x} \right|^2 dx \\ &= \tilde{I} + \tilde{II} + \tilde{III}. \end{aligned}$$

It follows from (3.14) that

$$\tilde{I} = \int_0^y \cos^2(kx) |e^{iky} - e^{ikz}|^2 dx \leq 2k^4(y - z)^2, \tag{3.15}$$

$$\tilde{II} = \int_y^z |i \sin(ky)e^{ikx} - \cos(kx)e^{ikz}|^2 dx \leq 4|y - z|, \tag{3.16}$$

$$\tilde{III} = \int_z^1 |i \sin(ky)e^{ikx} - i \sin(kz)e^{ikx}|^2 dx \leq k^4(y - z)^2. \tag{3.17}$$

Combining the above three inequalities, we obtain the desired estimate (3.10). □

Now we establish an error estimate between  $u$  and  $u^s$ .

**Theorem 3.4** *Let  $u$  and  $u^s$  be the solutions of (1.1) and (3.3), respectively. We have*

$$E(|u - u^s|_1^2) \leq (3k^4 + 4)h. \tag{3.18}$$

*Proof* By combining (3.7) with (3.8), we observe that

$$\begin{aligned} u' - (u^s)' &= \int_0^1 \frac{\partial G(x, y)}{\partial x} \dot{W}(y) dy - \int_0^1 \frac{\partial G(x, y)}{\partial x} \dot{W}^s(y) dy \\ &= \sum_{I_j \in T_h} \left[ \int_{I_j} \frac{\partial G(x, y)}{\partial x} dW(y) - |I_j|^{-1} \int_{I_j} \frac{\partial G(x, z)}{\partial x} dz \int_{I_j} 1 dW(y) \right] \\ &= \sum_{I_j \in T_h} \int_{I_j} \int_{I_j} |I_j|^{-1} \left( \frac{\partial G(x, y)}{\partial x} - \frac{\partial G(x, z)}{\partial x} \right) dz dW(y). \end{aligned} \tag{3.19}$$

Applying Itô's isometry yields

$$\begin{aligned} E(|u - u^s|_1^2) &= E\left(\int_0^1 \left[ \sum_{I_j \in T_h} \int_{I_j} \int_{I_j} |I_j|^{-1} \left( \frac{\partial G(x, y)}{\partial x} - \frac{\partial G(x, z)}{\partial x} \right) dz dW(y) \right]^2 dx\right) \\ &= \int_0^1 \sum_{I_j \in T_h} \int_{I_j} \int_{I_j} |I_j|^{-1} \left( \frac{\partial G(x, y)}{\partial x} - \frac{\partial G(x, z)}{\partial x} \right)^2 dz dy dx. \end{aligned}$$

It follows from the Hölder inequality that

$$\begin{aligned} E(|u - u^s|_1^2) &\leq \int_0^1 \sum_{I_j \in T_h} |I_j|^{-1} \int_{I_j} \int_{I_j} \left( \frac{\partial G(x, y)}{\partial x} - \frac{\partial G(x, z)}{\partial x} \right)^2 dz dy dx \\ &= \sum_{I_j \in T_h} |I_j|^{-1} \int_{I_j} \int_{I_j} \int_0^1 \left( \frac{\partial G(x, y)}{\partial x} - \frac{\partial G(x, z)}{\partial x} \right)^2 dx dz dy. \end{aligned} \tag{3.20}$$

Then the desired result (3.18) follows from (3.10) and (3.20). □

#### 4 Finite volume method for the stochastic Helmholtz equation in one-dimension

In this section, we consider the finite volume approximation of variational problem (3.4) and establish its error estimates.

The linear finite volume approximation to (3.4) is: Find  $u_h^s = \sum_{m=1}^n u_m^s \phi_m(x)$  such that

$$a(u_h^s, \psi_j) = (g, \psi_j) + (\dot{W}^s, \psi_j), \quad j = 1, 2, \dots, n. \tag{4.1}$$

The approximate variational problem (4.1) has a unique solution. The following theorem presents an error estimate for  $u - u_h^s$ .

**Theorem 4.1** *Let  $u$  and  $u_h^s$  be the solutions of (1.1) and (4.1), respectively. If  $kh$  is small enough, then we have*

$$E(|u - u_h^s|_1^2) \leq 2(3k^4 + 4)h + CC_5(1 + k^2h)^2h. \tag{4.2}$$

*Proof* By (2.31), (3.5), (3.18) and the triangle inequality, we have that

$$\begin{aligned} E(|u - u_h^s|_1^2) &\leq 2E(|u - u^s|_1^2) + 2E(|u^s - u_h^s|_1^2) \\ &\leq 2(3k^4 + 4)h + C(1 + k^2h)^2 h^2 E(|u^s|_2^2) \\ &\leq 2(3k^4 + 4)h + CC_5(1 + k + k^2)^2 h, \end{aligned}$$

which leads to the desired result. □

### 5 Numerical experiments

In this section, we present numerical examples to demonstrate our theoretical results in the previous section. All the experiments are performed with Matlab 7v on an Intel Xeon (4-core) with 3.60 GHz and 16 GB RAM.

#### 5.1 Problem 1

Consider the deterministic Helmholtz equation

$$\begin{cases} -\frac{d^2u}{dx^2} - k^2u(x) = -1, & x \in (0, 1), \\ u(0) = 0, & u'(1) - iku(1) = 0. \end{cases} \tag{5.1}$$

The exact solution of the above problem is

$$u = \frac{1}{k^2} [-\sin k \sin(kx) - \cos(kx) + 1 + i \sin(kx)(\cos k - 1)].$$

We use this problem to measure the accuracy for two schemes, including the linear FVM and FEM. The error is measured in the relative discrete  $L_2$ -norm and the relative discrete  $H^1$ -seminorm. In details, the discrete  $L_2$ -norm and  $H^1$ -seminorm are respectively defined as: for any complex vector  $\mathbf{z} = [z_0, z_1, \dots, z_M]$ ,

$$\|z\|_0^2 := \sum_{j=0}^M h|z_j|^2, \quad |z|_1^2 := \sum_{j=1}^M h \left| \frac{z_j - z_{j-1}}{h} \right|^2,$$

where  $|z_j|$  is the complex modulus of  $z_j$ . Let  $u$  and  $u_h$  denote the exact and numerical solutions, respectively. Then, the relative discrete  $L_2$ -norm is defined as  $\frac{\|u - u_h\|_0}{\|u\|_0}$ . The relative discrete  $H^1$ -seminorm is defined in a similar way.

Tables 1, 2 and 3 show the error in the relative discrete  $L_2$ -norm for two different schemes with different gridpoints  $N$  for  $k = 30, 200, 500$ , respectively. We find that, for both the linear FVM and FEM, the rate of convergence for the error in the relative discrete  $L_2$ -norm is of order 2, as expected. In addition, Tables 4, 5 and 6 show the error in the relative discrete  $H^1$ -seminorm for two different schemes with different gridpoints  $N$  for  $k = 30, 200, 500$ , respectively. It is easy to see that, for both schemes, the rate of convergence for the error in the relative discrete  $H^1$ -seminorm is of order 2. In particular, from these six tables, we see that the error for the linear FVM is only half of that for the linear FEM, which verifies the relations between  $k^N$  and  $k$  for the two methods as presented previously in (2.54) and (2.57).

**Table 1** The error in the relative discrete  $L_2$ -norm for problem (5.1) with  $k = 30$

$n$	32	64	128	256	512	1024
linear FEM	0.6719	0.1667	0.0409	0.0102	0.0025	6.3335e-004
linear FVM	0.2964	0.0783	0.0197	0.0049	0.0012	3.0847e-004

**Table 2** The error in the relative discrete  $L_2$ -norm for problem (5.1) with  $k = 200$

$n$	512	1024	2048	4096	8192	16,384
linear FEM	0.8194	0.1862	0.0440	0.0108	0.0027	6.7253e-004
linear FVM	0.3852	0.0893	0.0217	0.0054	0.0013	3.3556e-004

**Table 3** The error in the relative discrete  $L_2$ -norm for problem (5.1) with  $k = 500$

$n$	2048	4096	8192	16,384	32,768	65,536
linear FEM	0.8107	0.2235	0.0557	0.0139	0.0035	8.6743e-004
linear FVM	0.4402	0.1114	0.0278	0.0069	0.0017	4.3288e-004

**Table 4** The error in the relative discrete  $H^1$ -seminorm for problem (5.1) with  $k = 30$

$n$	32	64	128	256	512	1024
linear FEM	0.8555	0.2157	0.0533	0.0133	0.0033	8.2684e-004
linear FVM	0.3789	0.1014	0.0257	0.0064	0.0016	4.0242e-004

**Table 5** The error in the relative discrete  $H^1$ -seminorm for problem (5.1) with  $k = 200$

$n$	512	1024	2048	4096	8192	16,384
linear FEM	1.1484	0.2616	0.0618	0.0152	0.0038	9.4538e-004
linear FVM	0.5406	0.1254	0.0305	0.0076	0.0019	4.7169e-004

**Table 6** The error in the relative discrete  $H^1$ -seminorm for problem (5.1) with  $k = 500$

$n$	2048	4096	8192	16,384	32,768	65,536
linear FEM	0.9649	0.2663	0.0664	0.0166	0.0041	0.0010
linear FVM	0.5242	0.1327	0.0331	0.0083	0.0021	5.1575e-004

**Table 7** The error in the relative discrete  $L_2$ -norm for problem (5.1) with  $kh = 0.125$

$k$	200	300	400	500	600	700
linear FEM	0.0730	0.1278	0.1832	0.2344	0.2776	0.3085
linear FVM	0.0358	0.0626	0.0903	0.1169	0.1406	0.1595

**Table 8** The error in the relative discrete  $H^1$ -seminorm for problem (5.1) with  $kh = 0.125$

$k$	200	300	400	500	600	700
linear FEM	0.1026	0.1644	0.2238	0.2791	0.3284	0.3685
linear FVM	0.0503	0.0805	0.1103	0.1392	0.1664	0.1905

Further comparison between the linear FEM and FVM is given in Tables 7 and 8. Table 7 presents the error in the relative discrete  $L_2$ -norm of two schemes for the case  $kh = 0.125$ , and Table 8 shows the corresponding error in the relative discrete  $H^1$ -seminorm. The wavenumber  $k$  in the two tables varies from 200 to 700. As seen from these two tables,

the accuracy of the linear FVM is higher than that of the linear FEM, and it deteriorates much slower if  $kh$  is chosen to be a constant.

### 5.2 Problem 2

We solve the deterministic Helmholtz problem

$$\begin{cases} -\frac{d^2u}{dx^2} - k^2u(x) = 40 \cos(4x) + 80i \sin(3x), & x \in (0, 1), \\ u(0) = 0, & u'(1) - iku(1) = 0. \end{cases} \tag{5.2}$$

The above problem's exact solution is:

$$\begin{aligned} u(x) = & \frac{1}{k} \left\{ 20 \sin(kx) \left[ \frac{1}{k+4} (\sin(k+4) - \sin((k+4)x)) \right. \right. \\ & \left. \left. + \frac{1}{k-4} (\sin(k-4) - \sin((k-4)x)) \right] \right. \\ & + 40i \sin(kx) \left[ \frac{1}{3+k} (\cos((3+k)x) - \cos(3+k)) \right. \\ & \left. \left. + \frac{1}{3-k} (\cos((3-k)x) - \cos(3-k)) \right] \right. \\ & + 40i \cos(kx) \left[ \frac{\sin((k-3)x)}{k-3} - \frac{\sin((k+3)x)}{k+3} \right] \\ & - 40 \sin(kx) \left[ \frac{\sin(k-3)}{k-3} - \frac{\sin(k+3)}{k+3} \right] \\ & \left. \left. + 20 \cos(kx) \left[ \frac{1}{k+4} (1 - \cos((k+4)x)) + \frac{1}{k-4} (1 - \cos((k-4)x)) \right] \right] \right. \\ & \left. \left. + 20i \sin(kx) \left[ \frac{1}{k+4} (1 - \cos(k+4)) + \frac{1}{k-4} (1 - \cos(k-4)) \right] \right] \right\}. \end{aligned}$$

By this problem, the accuracy of the linear FVM and FEM are also measured in the relative discrete  $L_2$ -norm and the relative discrete  $H^1$ -seminorm.

Tables 9 and 10 show the error in the relative discrete  $L_2$ -norm for two different schemes with different gridpoints  $N$  for  $k = 30, 300$ , respectively. In addition, Tables 11 and 12 show the error in the relative discrete  $H^1$ -seminorm for two different schemes with different gridpoints  $N$  for  $k = 30, 300$ , respectively. From these four tables, we know that for both the linear FVM and FEM, the convergence rate of the error in the relative discrete  $L_2$ -norm or the relative discrete  $H^1$ -seminorm is 2. Furthermore, seen from Tables 9–12, we find that the error for the linear FVM is only half of that for the linear FEM, which is an interesting result. This confirms the efficiency of the linear FVM.

**Table 9** The error in the relative discrete  $L_2$ -norm for problem (5.2) with  $k = 30$

$n$	32	64	128	256	512	1024
linear FEM	0.2067	0.0761	0.0209	0.0053	0.0013	3.3532e-004
linear FVM	0.1332	0.0425	0.0112	0.0028	7.1319e-004	1.7837e-004

**Table 10** The error in the relative discrete  $L_2$ -norm for problem (5.2) with  $k = 300$

$n$	1024	2048	4096	8192	16,384	32,768
linear FEM	0.2270	0.0817	0.0220	0.0056	0.0014	3.5200e-004
linear FVM	0.1455	0.0431	0.0112	0.0028	7.0731e-004	1.7692e-004

**Table 11** The error in the relative discrete  $H^1$ -seminorm for problem (5.2) with  $k = 30$

$n$	32	64	128	256	512	1024
linear FEM	0.4094	0.1532	0.0422	0.0108	0.0027	6.8063e-004
linear FVM	0.2649	0.0852	0.0226	0.0057	0.0014	3.6075e-004

**Table 12** The error in the relative discrete  $H^1$ -seminorm for problem (5.2) with  $k = 300$

$n$	1024	2048	4096	8192	16,384	32,768
linear FEM	0.4452	0.1603	0.0432	0.0110	0.0028	6.9091e-004
linear FVM	0.2853	0.0846	0.0220	0.0055	0.0014	3.4726e-004

### 5.3 Problem 3

We consider the stochastic Helmholtz equation

$$\begin{cases} -\frac{d^2u}{dx^2} - k^2u(x) = -1 + \dot{W}(x), & x \in (0, 1), \\ u(0) = 0, & u'(1) - ik u(1) = 0. \end{cases} \tag{5.3}$$

When white noise is absent, the above problem reduces to Problem 1. We will use the random number generator to simulate the Gaussian random process  $\dot{W}^s$ . Furthermore, we shall follow [8] to evaluate  $E(u_h^s)$  by using the Monte Carlo method when examining

$$e_1(h) := |E(u) - E(u_h^s)|_1,$$

to ensure that we have used enough samples. Notice that it is impossible to evaluate  $E(|u - u_h^s|_1^2)$ , since it is impossible obtain an explicit expression for  $u$ . We also employ the following type of error:

$$e_2(h) := |E(|u|_1^2) - E(|u_h^s|_1^2)|$$

to check the error estimates for the finite volume method. By a simple computation, we have

$$\begin{aligned} E(u) &= \frac{1}{k^2} [-\sin k \sin(kx) - \cos(kx) + 1 + i \sin(kx)(\cos k - 1)], \\ E(|u|_1^2) &= \int_0^1 \left\{ \left| \int_0^1 -\frac{\partial G(x,y)}{\partial x} dy \right|^2 + \int_0^1 \left| \frac{\partial G(x,y)}{\partial x} \right|^2 dy \right\} dx \\ &= \frac{1}{2} + \frac{1}{k^2} \left[ \frac{3}{2} - \cos k + \frac{1}{4k} \sin(2k) - \frac{1}{k} \sin k \right]. \end{aligned}$$

When  $k = 1$ ,  $E(|u|_1^2) = 0.8456$ . In addition,  $E(|u|_1^2) = 0.5157$  for  $k = 6$ , and  $E(|u|_1^2) = 0.5047$  for  $k = 12$ .

**Table 13** The linear FVM for problem (5.3) with  $k = 1$

$h$	$e_1$	Rate	$E( u_h^s _1^2)$	$e_2$	Rate
1/2	0.0101		0.6380	0.2076	
1/4	0.0045	1.1664	0.7718	0.0738	1.4921
1/8	0.0029	0.6339	0.8032	0.0424	0.7996
1/16	0.0013	1.1575	0.8270	0.0186	1.1888
1/32	4.8615e-004	1.4190	0.8385	0.0071	1.3894

**Table 14** The linear FVM for problem (5.3) with  $k = 6$

$h$	$e_1$	Rate	$E( u_h^s _1^2)$	$e_2$	Rate
1/3	0.0142		0.2369	0.2788	
1/6	0.0081	0.8099	0.3993	0.1164	1.2601
1/12	0.0027	1.5850	0.4719	0.0438	1.4101
1/24	0.0012	1.1699	0.4956	0.0201	1.1237
1/48	7.2862e-04	0.7198	0.5088	0.0068	1.5636

**Table 15** The linear FVM for problem (5.3) with  $k = 12$

$h$	$e_1$	Rate	$E( u_h^s _1^2)$	$e_2$	Rate
1/8	0.0209		0.2739	0.2309	
1/16	0.0070	1.5781	0.4332	0.0715	1.6913
1/32	0.0035	1	0.4803	0.0244	1.5511
1/64	0.0013	1.4288	0.4949	0.0098	1.3160
1/128	7.3070e-04	0.8312	0.5023	0.0024	2.0297

The computational results of the linear FVM approximations for (5.3) with  $k = 1, 6, 12$  are displayed in Tables 13, 14 and 15, respectively. The third columns of the tables show that the convergence rate for  $E(u_h^s)$  is of order 1, which confirms our theoretical result presented in the previous section. The sixth columns of the tables show that the rate of convergence for  $E(|u_h^s|_1^2)$  is of order 1 as expected, which implies that our sample sizes are good enough to ensure the accuracy of the Monte Carlo method.

### 6 Conclusions

In this paper, we proposed the linear FVM for the stochastic Helmholtz equation, driven by an additive white noise forcing term in one-dimension. Firstly, the linear FVM for the deterministic Helmholtz equation in one-dimension was presented, and then its solution's existence and uniqueness were considered. For the linear FVM, its solution's error estimate in  $H^1$ - and  $L_2$ -norm were established. Moreover, its dispersion equation was presented, and the error between the numerical and exact wavenumbers was analyzed. We also made comparisons between the linear FVM and FEM. Theoretical analysis and practical computations indicated that the error for the linear FVM is only half of that for the linear FEM. By means of approximating the white noise by a piecewise constant process, we converted the stochastic Helmholtz equation into the deterministic Helmholtz equation, which is an approximate problem for the stochastic Helmholtz problem. The regularity of the solution for the approximate problem was discussed, and its error estimates in  $H^1$ -norm were presented. Furthermore, the linear FVM was applied for solving this approximate problem, and the  $H^1$  error estimates between the finite volume solutions and the exact solution of the stochastic Helmholtz problem were obtained. Finally, numerical experiments were given to verify our theoretical results.

### Acknowledgements

The authors would like to thank Prof. Zhongying Chen in Sun Yat-Sen University for valuable comments, which led to a much better version of this article.

### Funding

This research is partially supported by a project of Shandong Province Higher Educational Science and Technology Program of China under the grant J18KA221, the Natural Science Foundation of China under grants 11301310, 11471196 and 11771257.

### Competing interests

The authors declare that they have no competing interests.

### Authors' contributions

All authors contributed equally to the manuscript. All authors read and approved the final manuscript.

### Author details

<sup>1</sup>School of Mathematics and Statistics, Qilu University of Technology (Shandong Academy of Sciences), Jinan, P.R. China.

<sup>2</sup>School of Mathematics and Statistics, Shandong Normal University, Jinan, P.R. China.

### Publisher's Note

Springer Nature remains neutral with regard to jurisdictional claims in published maps and institutional affiliations.

Received: 11 October 2018 Accepted: 7 February 2019 Published online: 01 March 2019

### References

1. Allen, E.J., Novosel, S.J., Zhang, Z.: Finite element and difference approximation of some linear stochastic partial differential equations. *Stoch. Stoch. Rep.* **64**, 117–142 (1998)
2. Babuška, I., Ihlenburg, F., Paik, E.T., Sauter, S.A.: A generalized finite element method for solving the Helmholtz equation in two dimensions with minimal pollution. *Comput. Methods Appl. Math.* **128**, 325–359 (1995)
3. Babuška, I., Sauter, S.A.: Is the pollution effect of the FEM avoidable for the Helmholtz equation considering high wave numbers? *SIAM Rev.* **42**, 451–484 (2000)
4. Bao, G., Chen, C., Li, P.: Inverse random source scattering problems in several dimensions. *SIAM/ASA J. Uncertain. Quantificat.* **4**, 1263–1287 (2016)
5. Bao, G., Chow, S.-N., Li, P., Zhou, H.: Numerical solution of an inverse medium scattering problem with a stochastic source. *Inverse Probl.* **26**, 074014 (2010)
6. Bao, G., Chow, S.-N., Li, P., Zhou, H.: An inverse random source problem for the Helmholtz equation. *Math. Comput.* **83**, 215–233 (2014)
7. Cao, Y., Yang, H., Yin, L.: Finite element methods for semilinear elliptic stochastic partial differential equations. *Numer. Math.* **106**, 181–198 (2007)
8. Cao, Y., Zhang, R., Zhang, K.: Finite element and discontinuous Galerkin method for stochastic Helmholtz equation in two- and three-dimensions. *J. Comput. Math.* **26**, 702–715 (2008)
9. Chen, Z., Cheng, D., Feng, W., Wu, T.: An optimal 9-point finite difference scheme for the Helmholtz equation with PML. *Int. J. Numer. Anal. Model.* **10**, 389–410 (2013)
10. Chen, Z., Xu, Y., Zhang, J.: A second-order hybrid finite volume method for solving the Stokes equation. *Appl. Numer. Math.* **119**, 213–224 (2017)
11. Chen, Z., Xu, Y., Zhang, Y.: A construction of higher-order finite volume methods. *Math. Comput.* **84**, 599–628 (2015)
12. Du, Q., Zhang, T.: Numerical approximation of some linear stochastic partial differential equations driven by special additive noises. *SIAM J. Numer. Anal.* **40**, 1421–1445 (2002)
13. Ewing, R.E., Lin, T., Lin, Y.: On the accuracy of the finite volume element method based on piecewise linear polynomials. *SIAM J. Numer. Anal.* **39**, 1865–1888 (2002)
14. Feng, X., Wu, H.: Discontinuous Galerkin methods for the Helmholtz equation with large wave number. *SIAM J. Numer. Anal.* **47**, 2872–2896 (2009)
15. Ihlenburg, F., Babuška, I.: Finite element solution of the Helmholtz equation with high wave number. Part I: the  $h$ -version of the FEM. *Comput. Math. Appl.* **30**, 9–37 (1995)
16. Ishimaru, A.: *Wave Propagation and Scattering in Random Media*. Academic Press, New York (1978)
17. Jo, C.-H., Shin, C., Suh, J.H.: An optimal 9-point, finite-difference, frequency-space, 2-D scalar wave extrapolator. *Geophysics* **61**, 529–537 (1996)
18. Li, P.: An inverse random source scattering problem in inhomogeneous media. *Inverse Probl.* **27**, 035004 (2011)
19. Li, R., Chen, Z., Wu, W.: *Generalized Difference Methods for Differential Equations: Numerical Analysis of Finite Volume Methods*. Dekker, New York (2000)
20. Mysak, L.A.: Wave propagation in random media, with oceanic applications. *Rev. Geophys.* **16**, 233–261 (1978)
21. Trefethen, L.N.: Group velocity in finite difference schemes. *SIAM Rev.* **24**, 113–136 (1982)
22. Turkel, E., Gordon, D., Gordon, R., Tsynkov, S.: Compact 2D and 3D sixth order schemes for the Helmholtz equation with variable wave number. *J. Comput. Phys.* **232**, 272–287 (2013)
23. Walsh, J.B.: An introduction to stochastic partial differential equations. In: *École d'Été de Probabilités de Saint Flour XIV—1984*, pp. 265–439. Springer, Berlin (1986)
24. Wu, T.: A dispersion minimizing compact finite difference scheme for the 2D Helmholtz equation. *J. Comput. Appl. Math.* **311**, 497–512 (2017)
25. Wu, T., Xu, R.: An optimal compact sixth-order finite difference scheme for the Helmholtz equation. *Comput. Math. Appl.* **75**, 2520–2537 (2018)
26. Yuste, R.: Fluorescence microscopy today. *Nat. Methods* **2**, 902–905 (2005)
27. Zhang, Z., Karniadakis, G.E.: *Numerical Methods for Stochastic Partial Differential Equations with White Noise*. Springer, Berlin (2017)